



Significant improvements in mechanical properties of AA5083 aluminum alloy using dual equal channel lateral extrusion

N. FAKHAR¹, F. FERESHTEH-SANIEE¹, R. MAHMUDI²

1. Department of Mechanical Engineering, Faculty of Engineering, Bu-Ali Sina University, Hamedan 65178, Iran;

2. School of Metallurgical and Materials Engineering, College of Engineering, University of Tehran, Tehran, Iran

Received 22 November 2015; accepted 27 September 2016

Abstract: Dual equal channel lateral extrusion (DECLE), as a severe plastic deformation (SPD) process, was employed for improving the mechanical properties of AA5083 aluminum alloy. Several experiments were conducted to study the influences of the route type, namely A and B, and pass number on mechanical properties of the material. The process was conducted up to 6 passes with decreasing process temperature, specifically from 573 to 473 K. Supplementary experiments involving metallography, hardness and tensile tests were carried out in order to evaluate the effects of the process variables. The hardness measurements exhibited reasonably uniform distributions within the product with a maximum increase of 64% via a 6-pass operation. The yield and ultimate strengths also amended 107% and 46%, respectively. These significant improvements were attributed to the severe shear deformation of grains and decreasing pass temperature, which intensified the grain refinement. TEM images showed an average grain size reduction from 100 μm for the annealed billet to 200 nm after 6 passes of DECLE. Finally, the experimental findings for routes A and B were compared and discussed and some important conclusions were drawn.

Key words: AA5083 aluminum alloy; severe plastic deformation; dual equal channel lateral extrusion; hardness homogeneity

1 Introduction

Production of ultra-fine and nano-structured materials by means of severe plastic deformation (SPD) techniques has attracted many researchers during the last decade. These methods are capable of providing superior mechanical properties, namely; high yield and ultimate strengths, extended fatigue life, and, in some cases, greater ductility at lower temperatures [1]. SPD techniques could also be implemented for a wide range of materials including structural and functional materials. Besides structural materials, ultrafine, nanocrystal and amorphous microstructures could be created in shape memory alloys as functional materials [2–5]. Several SPD methods have been proposed, which can be divided into four categories based on the geometry of the specimen. Some of the SPD techniques such as equal channel angular pressing (ECAP) [6], cyclic extrusion compression (CEC) [7], cyclic expansion extrusion (CEE) [8], twist extrusion (TE) [9], and simple shear extrusion (SSE) [10] are employed for inducing high strains into the rods. On the other hand, several operations including

high pressure torsion (HPT) [11], accumulative roll bonding (ARB) [12], repetitive corrugation and straightening (RCS) [13], high ratio different speed rolling (HRDSR) [14] and equal channel angular rolling (ECAR) [15] have been introduced for production of fine grain sheets. The mechanical properties of tubes can also be improved by means of processes such as tube channel angular pressing (TCAP) [16], high pressure tube twisting (HPTT) [17], tube channel pressing (TCAP) [18] and tube high pressure shearing (T-HPS) [19]. Finally, two operations, namely ECAP of plates [20] and repetitive upsetting (RU) [21] were proposed for production of plates with fine-grain structures. The latter process was firstly introduced with another appellation, namely dual equal channel lateral extrusion (DECLE) [22]. Among the above mentioned SPD processes, ECAP operation is the most applicable and effective technique for refining the structures of different materials. The inherent attractiveness and advantages of this process have resulted in development of some new SPD methods, such as TCAP, ECAR and T-shaped equi-channel angular pressing (T-ECAP) [23].

The DECLE process is one of the operations

proposed based on the principles of the ECAP method and is employed for refining the microstructure of the plates [24]. TALEBANPOUR et al [22] initially suggested this technique and then, GUO et al [21] named the operation as the repetitive upsetting and used it for refining the microstructure of disks and rectangular plates. To perform the process, the billet is first located in the vertical region of a T-shaped channel. Then, the punch pushes the billet into the horizontal channel of the die set. The principles of this SPD technique are very similar to those of T-ECAP proposed by RAO et al [23] for modification of mechanical properties of bars with rectangle sections. Compared with ECAP and T-ECAP, DECLE process involves several advantages such as [21,22]:

- 1) The length and width of the specimen are equal. Therefore, it is possible to rotate the sample in various directions after each pass of the process. This feature results in a better distribution of shear deformation in perpendicular directions, and consequently, different routes can be employed for performing the SPD operation.

- 2) This process is a combination of ECAP and multi-directional forging (MDF), because the transverse flow of the material is restricted, whereas the flow occurs in the other two directions. Hence, a more uniform deformation of the specimen can be resulted.

- 3) The operation involves greater strains during each pass and needs lower forming load, compared with the ECAP method.

- 4) DECLE is capable of producing thick and quite large plates with fine-grained structure and improved mechanical properties.

The above advantages have recently made the DECLE process attractive to researchers and industries. This process is as easy as ECAP to perform but with more benefits. Since the DECLE technique has just recently been introduced and only some limited researches have been conducted regarding this process, doing more investigations is important and beneficial to discover its potentials. With this regard, more features of the operation have been evaluated in the present work and detailed information on the levels of hardness and the degrees of homogeneity on three orthogonal planes has been achieved. In the present research work, DECLE process was applied to AA5083 aluminum alloy in two different routes and up to six passes. The operation was carried out with decreasing temperature, such that the process temperature was reduced from 573 K for the first pass to 473 K for the sixth pass. Reduction in the temperature and induction of high and severe strains into the work-piece were two important variables affecting the microstructure modification and improvement in the mechanical properties of the alloy. The main goals of this

investigation were studying the influences of these variables on the microstructure and mechanical properties of AA5083 aluminum alloy and, also, inspection of hardness homogeneity through the processed material. For different test conditions, the microstructure of the alloy was observed by means of a transmission electron microscope (TEM). Tensile and microhardness tests were also conducted in order to evaluate the improvements in the strength and hardness of the deformed specimen and to examine uniformity of mechanical properties in the product.

2 Principles of DECLE

Figure 1 shows a schematic illustration of DECLE process. The specimens of this operation have equal length and width, but a different thickness. Each sample is first placed in the vertical channel with width and thickness equal to those of the specimen. The pressing punch forces the material to flow into a double sided horizontal channel with a cross section equal to those of the billet and the vertical channel. The metal flow in any other direction is completely constrained by the walls of the vertical and horizontal channels. The DECLE process can be imagined as a double sided ECAP operation or two back-to-back ECAP processes. In a DECLE operation, the specimen is simultaneously subjected to shear, compression and extrusion. The shear strain is mainly exerted to the sample at the junction of two channels. The strains due to compression and extrusion are applied to the deforming material between the punch and the horizontal channel. The dimensions of two channels are equal. Therefore, the dimensions of the product are the same as those of the billet and, as a consequence, the process can be repeated with various routes. There are two routes for DECLE, namely routes A and B. In route A, the sample is rotated 90° about Y

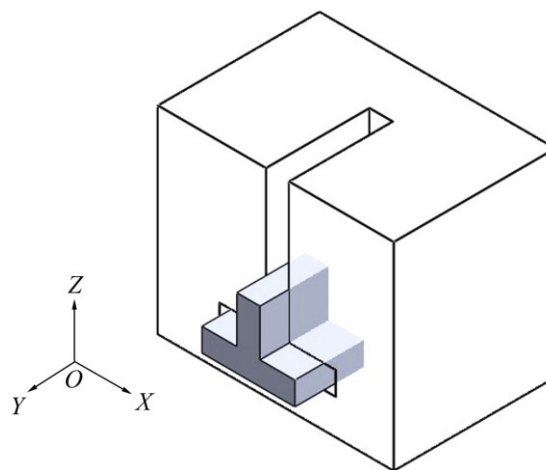


Fig. 1 Solid model of die set and specimen for typical DECLE process

axis (in Fig. 1) for the next pass, whereas in route B, the specimen is first turned 90° about the X axis and then 90° about the Z axis [22].

As mentioned above, DECLE process can be considered as a couple of back-to-back ECAP operations. In an ECAP process, the channels are perpendicular to each other and the inner (ϕ) and outer (ψ) angles between the channels are 90° and 0° , respectively, the induced strain during each pass is about 1.15 [25]. However, upper bound analysis of DECLE method [26] revealed an induced strain of 1.44 for each pass, i.e., 25% greater than ECAP. Similarity between the routes of DECLE and ECAP processes can also be established. For example, route A in DECLE is similar to routes A and C in ECAP process. On the other hand, routes B_{AZ} and B_{CZ} in ECAP [20] can be transformed into route B in DECLE operation. These similarities are beneficial when the performances and efficiencies of these two SPD techniques are compared.

3 Experimental

Commercially rolled AA5083 aluminum alloy (Al–4.2%Mg–0.63%Mn–0.18%Fe) plate having a nominal thickness of 20 mm was used for preparation of the DECLE samples. The dimensions of each sample were 10 mm \times 50 mm \times 50 mm. Before the DECLE tests, the specimens were annealed at 773 K for 1 h. The experiments were carried out by means of a 2000 kN hydraulic press with a ram velocity of 3 mm/s. In order to decrease the interfacial friction at elevated temperatures, MoS₂ was employed as the lubricant. The heating of die and specimen was performed by several built-in heating elements. The process temperature was also monitored and controlled by using a thermocouple located at the junction of the vertical and horizontal channels.

To reduce the grain size as much as possible, it was decided to conduct the DECLE experiments with decreasing temperature for subsequent passes. For this reason, the temperature of each pass was 20 K lower than the previous one. To select the initial temperature for the tests, three process temperatures were tried, namely, 623, 573, and 523 K. Among these, the specimen deformed at 523 K had a deep crack. However, there was no problem with the other two initial temperatures. Hence, the starting temperature was chosen to be 573 K for all the DECLE experiments. These experiments were conducted for both routes A and B and up to 6 passes. But for route A, the specimen fractured at the end of 5th pass and it was impossible to perform the 6th pass for this route. On the other hand, it was possible to carry out the 6th pass for route B, although minor surface cracks were observed in the final product. Figure 2 illustrates the DECLE

products after the 5th and 6th passes for routes A and B, respectively. It is worthy to mention that the largest crack formed on the sample after pass 6 of route B was 0.5 mm in depth and 2.5 mm in width. Before hardness measurement and preparation of tensile test samples for this and all other RUed specimens, two 1 mm thick layers were wire-cut from their top and bottom surfaces. Therefore, all the minor cracks mentioned above were removed from the sample before conducting the complementary tests.

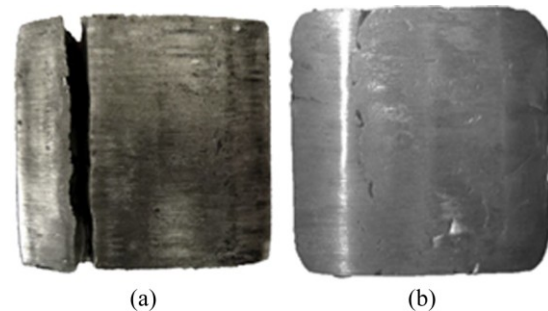


Fig. 2 Five-pass DECLED component using route A (a) together with typical 6-passed part obtained via route B (b)

It seems that underneath the plunger, the least strains are induced and a small dead zone exists. However, this is only the case for the 1st pass. During the next passes, this region experiences high strains and after several passes, a quite uniformly deformed product is obtained. Nevertheless, to avoid the influence of this zone on the result of the complementary mechanical tests, all the tensile and microhardness samples were prepared from regions far enough from this zone. The specimens for the tensile tests were prepared parallel to XY plane (Fig. 1) by using the wire-cut process. To evade the effects of the interfacial friction on the experimental results, before wire-cut machining of the tensile specimens, 1 mm thick layers were removed from top and bottom surfaces of the final DECLED part, as mentioned previously. The length, width and thickness of the gauge length of the tensile specimens were 4, 3 and 2 mm, respectively. The direction of force application was also considered to be parallel to Y axis (Fig. 1). All the tensile tests were conducted using a 50 kN servo-electrical testing machine with an initial strain rate of $1 \times 10^{-3} \text{ s}^{-1}$.

To examine the improvement and homogeneity in mechanical properties of the DECLED components, Vickers microhardness tests were performed after one pass for all the coordinate planes, namely, XY , XZ and YZ . However, to compare the results of different passes and routes, the hardness experiments were conducted only for plane YZ . These tests were carried out by applying 200 g for 20 s. Depending on the sizes of sections for

various coordinate planes, microhardness experiments were performed at points 1 or 2 mm apart from each other.

Both the optical and transmission electron microscopes were employed for studying the microstructures of the specimens DECLED under different test conditions. To observe micrographs with optical microscope, the samples were prepared using common metallurgical techniques and modified poulton's reagent as the etchant. The TEM specimens were produced parallel to XZ plane. To do so, 1 mm thick slices were cut using a low-speed saw. Then, they were mechanically polished to a thickness of 100 μm . Eventually, a disc 3 mm in diameter was punched from each slice for twin-jet electro polishing and thinning process at the room temperature.

4 Results and discussion

4.1 Microstructural studies

Figure 3 illustrates the coarse-grained structure of the AA5083 alloy before the DECLE operation. The average grain size was measured to be about 100 μm using the linear intercept method. The microstructural evolution of the alloy after the first pass of the process is shown in Fig. 4. This figure illustrates the deformation of grains next to the dead zone and in the YZ plane, where a large shear band can be seen in the micrograph. The formation of this band is due to severe localized flow between large columnar shaped grains [21]. As can be seen in Fig. 4(a), the shear band contains a filamentary structure, contrary to the outside regions which involve equi-axed grains. The presence of shear bands during the early passes of the ECAP operation of an Al–Mg alloy was previously reported [27]. Fracture of Al–Mg alloys due to concentration of plastic flow in narrow bands of severe shear deformation has also been observed [28]. The shear bands after the first pass of the DECLE process of other Mg alloys were also reported by the

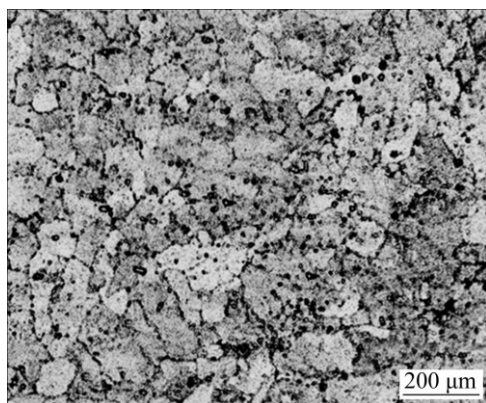


Fig. 3 Micrograph of annealed AA5083 aluminum alloy prior to DECLE process

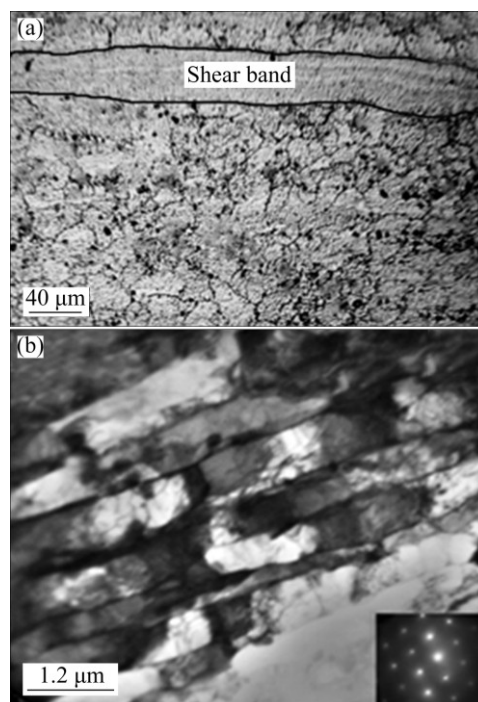


Fig. 4 Microstructure observations after first pass of DECLE operation at 573 K: (a) Optical micrograph of dead zone; (b) TEM image and corresponding SAED pattern from a zone far enough from dead zone

previous researchers [21,29].

In the present research work, using the circular intercept technique, the average grain size after the first pass of DECLE process was found to be 32 μm for the dead zone. The TEM image prepared after the first pass of the process and parallel to YZ plane is shown in Fig. 4(b). Grains with length of about 2.5 μm and widths of nearly 0.5 μm can be observed in this image. The SAED pattern contains clear points. This pattern illustrates that most of the fine grains created during the first pass of the operation involved low-angle boundaries. Similar situation was reported after the first pass of DECLE of pure aluminum [22]. After the first pass, in regions far enough from the dead zone, strains of about 1.5 are induced into the material, whereas the amount of deformation near the dead zone is much lower. That is why, a significant difference between the grain sizes of various regions of the one-pass DECLED part can be perceived. GUO et al [21] studied the microstructure of AZ31 magnesium alloy DECLED up to five passes through routes A and B. They found that among various passes of route A, after the first pass, there were slight differences between microstructural images of the YZ and XZ planes. For subsequent passes, no significant dissimilarity was observed between microstructures of material in these two coordinate planes. In other words, the greater the number of passes and induced strain, the more uniform the microstructure of the deformed

part [21].

TEM images together with the corresponding SAED patterns are shown in Fig. 5 after the 2nd, 4th and 6th passes through route B. These images are taken from the surfaces parallel to *XZ* plane. Due to 90° rotation of specimen about the *Z* axis for route B, the flow of metal during the second pass is perpendicular to that of the first pass. For this reason, the stretched microstructure after the first pass of the process is changed to equi-axed grains with an average size of 750 nm. Looking at the SAED pattern for the second pass, one can find more scattered points that are indicative of grains with high-angle boundaries. Going through the microstructure of the material after the 4th and 6th passes of route B,

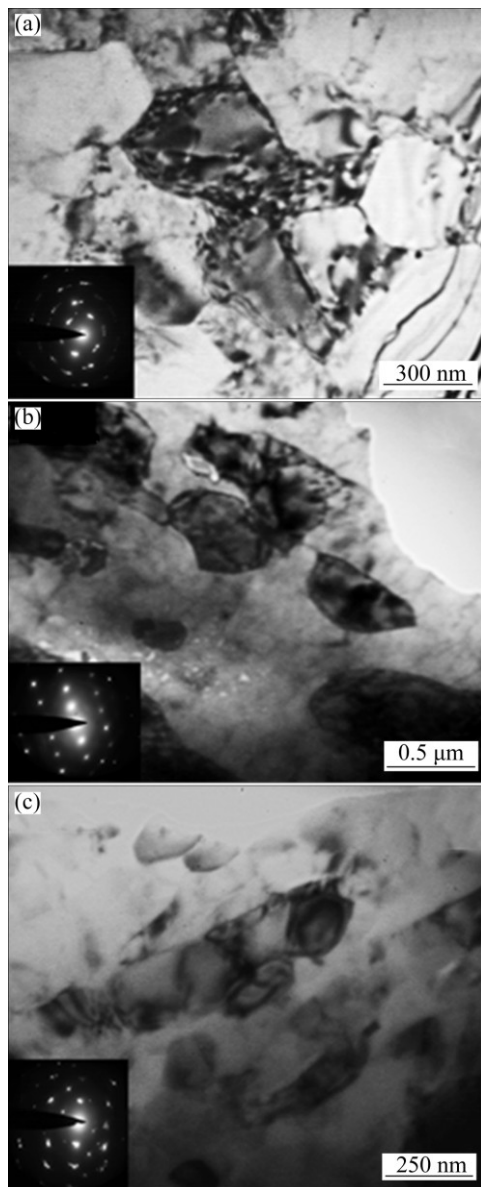


Fig. 5 TEM images and corresponding SAED patterns of alloy processed in different passes using route B: (a) After 2nd pass of DECLE operation; (b) After 4th pass of DECLE operation; (c) After 6th pass of DECLE operation

one can observe equi-axed grains with approximate average grain sizes of 400 and 200 nm, respectively. The number of rings in the relevant SAED patterns of these passes is increased and, as an indication of grains with high-angle boundaries, more scattered points can be detected in the patterns. It is worthy to mention that in this research work, the severe plastic deformation in the subsequent passes was accompanied with gradual reduction in the process temperature such that the 6th pass was conducted at 473 K. This situation intensified the reduction in the grain size and for a complete DECLE operation, the average grain size was reduced from 100 μm for the annealed billet to 200 nm after the 6th pass. A quite similar reduction was reported after 8 passes in route B_C of ECAP operation of Al–1.5%Mg alloy at room temperature, where the grain size decreased from 150 to 280 nm [30]. Although the starting temperature for DECLE experiments was 573 K in this investigation, because of progressive decrease in temperature, the grain size reduction was nearly the same as that achieved by 8-pass ECAP of this alloy at a constant temperature of 473 K for different passes of route C [31].

4.2 Mechanical properties

In order to examine the homogeneity of samples DECLED under various test conditions and to evaluate the improvements in their mechanical properties, many microhardness tests were performed on the *XY*, *XZ* and *YZ* planes (Fig. 1). Contour plots of the distributions of the hardness in these planes are illustrated in Fig. 6. As can be seen, slight variations occurred in the results, and for different points of the section, the microhardness changed within an acceptable and narrow range (please see the legends of Fig. 6). This uniformity in hardness distributions in various directions suggested the homogeneity of mechanical properties of the DECLE products. Calculation of the mean values for different planes resulted in average hardness numbers of HV 99.8, HV 99.6 and HV 99.3 for the *YZ*, *XZ* and *XY* coordinate planes, respectively. These findings imply that the hardness of the deformed material in various planes is almost the same.

The most inhomogeneity in properties of a severely deformed part is generally observed after the first pass of the process. Nevertheless, microhardness tests showed that even after the 1st pass of the DECLE operation, the homogeneity in hardness distributions of the deformed part in different directions is very good. KAMACHI et al [20] conducted 4 passes of ECAP with route B_C on pure aluminum plates at room temperature. They studied the microstructure and mechanical properties of the processed samples for all the three coordinate planes. Despite slight differences in microstructures in various

planes, they found an almost equal hardness in different directions.

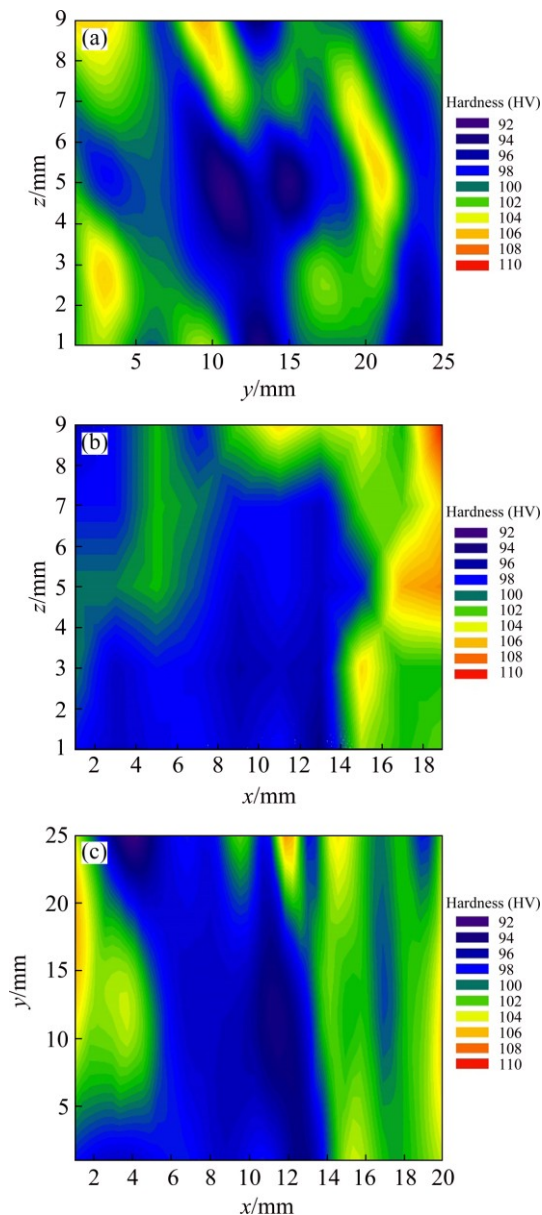


Fig. 6 Distributions of microhardness in planes XZ (a), YZ (b) and XY (c) after 1st pass of process

After the above preliminary study, to compare the hardness improvement of the alloy after various passes of the process, the hardness distribution was determined for plane YZ and in the Y direction. Figure 7 illustrates the results for both routes A and B. Minor fluctuations can again be seen in the experimental findings. As the induced strain is increased from 3 for the second pass to 9 for the sixth pass, the hardness gradually increases for both A and B routes. Based on Fig. 8, the hardness of the 6-pass DECLED with route B is 1.6 times that of the annealed billet. This significant improvement in hardness can be attributed to both severe plastic deformation and gradual reduction in temperature of the subsequent

passes, which have caused an ultra-fine microstructure. Hall–Petch relation suggests that the finer the grains of the alloy, the greater its hardness and strength. Figure 8 also shows that the hardness increase for route A is quite lower than that for route B. The hardness of material after the fourth pass of route A is almost equal to that of the second pass of route B, whereas the process temperature is 40 °C greater for the later conditions.

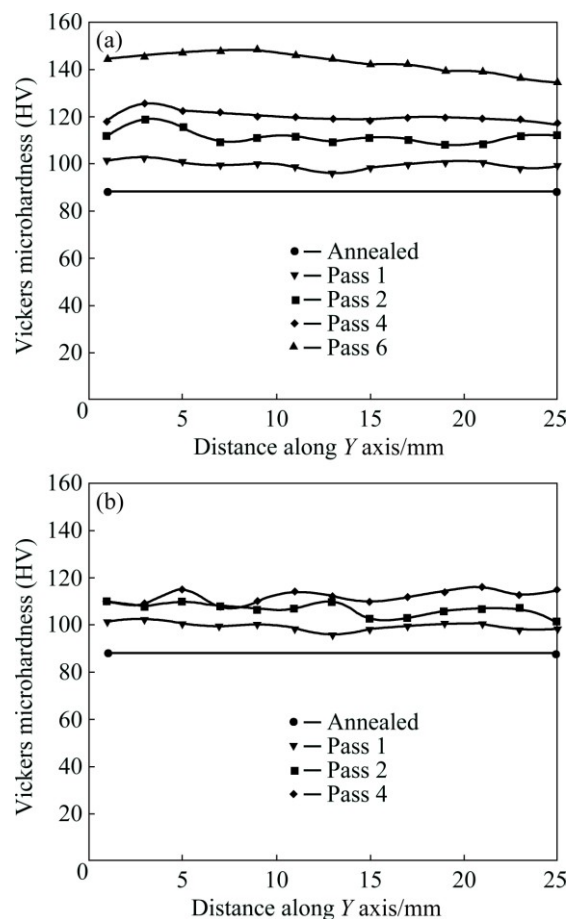


Fig. 7 Variations of hardness in plane YZ for components DECLED with various passes and using route A (a) and route B (b)

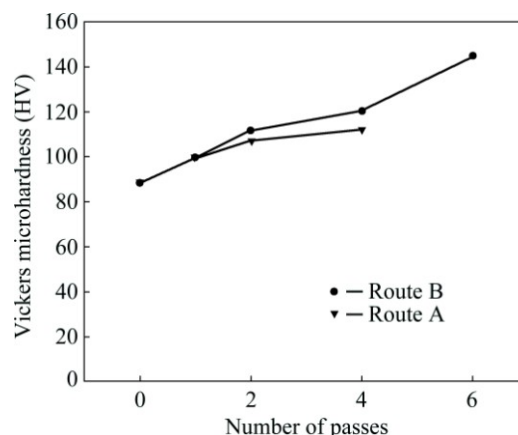


Fig. 8 Variations of average hardness with number of passes for different routes of DECLE process

An important point worthy to mention is the monotonic rise in the hardness of the alloy when the number of passes increases. This is in contrast to the observations made by CHANG et al [31]. They performed 8-pass ECAP process with AA5083 alloy at the constant temperature of 473 K. They found a significant improvement in hardness of the 1-passed sample, whereas no significant increase was observed after the subsequent passes of the operation. It was reported [31] that after the third pass of the ECAP process, a saturation in hardness of the material had occurred. They claimed that considerable improvement of hardness after pass one was due to strain hardening, which in turn, was a consequence of increase in dislocation density and formation of subgrain bands. All these were caused by shear deformation within the initial coarse grains of the material. Saturation of hardness after the next passes of ECAP was assigned to dynamic recovery, when the subgrains rotated and the dislocations rearranged [31]. This 8-pass ECAP process of AA5083 aluminum alloy increased its hardness from HV 80 to HV 110 [31]. However, in the present study, a 6-pass DECLE operation with the same alloy and using route B has changed the hardness of the material from HV 88 to HV 144. This experimental finding is comparable with that obtained by a 5-pass ECAP at room temperature for the same alloy, where the hardness increased from HV 80 for the billet to HV 155 for the 5-passed specimen [32]. However, it is obvious that this 5-pass ECAP operation at room temperature needs considerably more forming load and energy compared with similar process at elevated temperatures.

The engineering stress–strain (σ – ε) curves of the processed alloy obtained by tensile tests are shown in Figs. 9(a) and (b) for routes A and B, respectively. These figures indicate that both the yield stress (YS) and ultimate tensile strength (UTS) increased when the number of passes increased for both routes. The elongation as well as the YS and UTS of the DECLED alloy are compared in Table 1 for different routes and passes. Based on these experimental results, one can find out that improvement in both the yield and ultimate strengths of the material for route B is greater than that of route A, whereas the ductility enhancement is higher for route A, compared with route B. After the first pass of the process, although the ductility was not changed, YS and UTS were increased by 27% and 13%, respectively, compared with the annealed billet. After the second pass of route A, the elongation almost remained unchanged, whereas YS and UTS grew 36% and 18%, respectively, in comparison with the initial billet. However, a different situation occurred after the fourth pass of route A.

After this pass of DECLE operation, although the yield stress increased, the ultimate strength and

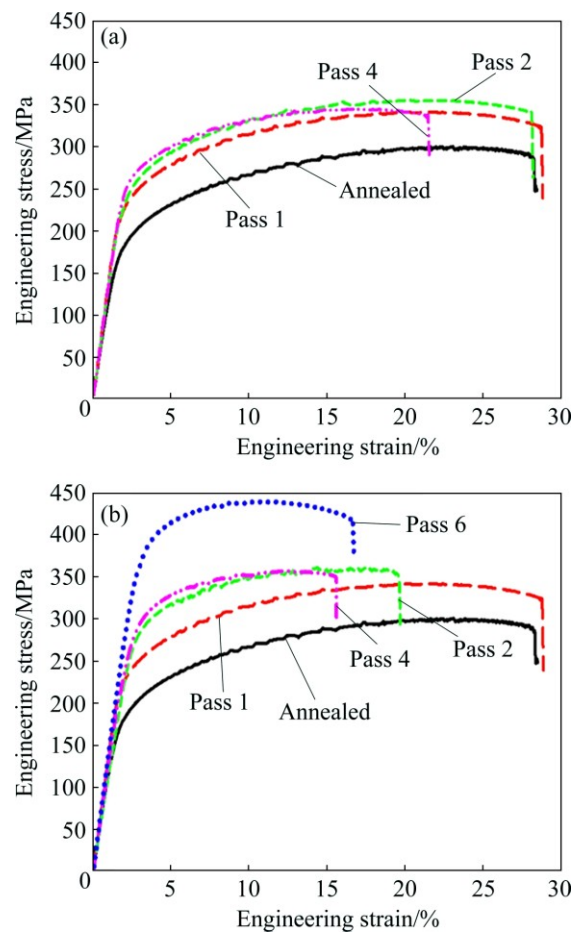


Fig. 9 Engineering stress–strain curves at room temperature for AA5083 alloy DECLED with different passes and using route A (a) and route B (b)

elongation decreased with respect to the second pass. The second, fourth and sixth passes of route B have, respectively, resulted in 56%, 63% and 107% improvements in YS, compared with its initial value. The respective enrichments in the ultimate strength were 20%, 18% and 46%, respectively. Similar to route A, in this route UTS slightly decreased from the second pass to the end of the fourth pass of the process. For route B, the elongation of AA5083 alloy gradually decreased as the number of passes increased, such that after the sixth pass the elongation reduced 42%, compared with unprocessed metal.

As an indication of the strain hardening capacity of an alloy, sometimes, the YS /UTS ratio is employed. The lower values of this ratio mean higher capacities for strain hardening behavior [33]. Table 1 summarizes the values of YS /UTS ratio for different passes and routes. Going through the results, one can conclude that, for both routes, the value of this ratio monotonically increases as the pass number and the induced strain increase. This increase of YS/UTS ratio is certainly more

Table 1 Yield strength (YS) and ultimate tensile strength (UTS) together with elongation of AA5083 components processed with different passes and routes

Number of pass	Route A				Route B			
	YS/MPa	UTS/MPa	YS/UTS	Elongation/%	YS/MPa	UTS/MPa	YS/UTS	Elongation/%
0 (Annealed)	180	300	0.60	28.7	180	300	0.60	28.7
1 ($T=573$ K)	230	341	0.67	28.7	230	341	0.67	28.7
2 ($T=553$ K)	245	355	0.69	28.2	280	360	0.77	19.6
4 ($T=513$ K)	260	345	0.75	21.5	294	356	0.82	17.7
6 ($T=473$ K)					372	438	0.85	16.6

evident for route B. Therefore, it can be deduced that the strain hardening behavior is more apparent for the material DECLED in route A. On the other hand, for route B by increasing the induced strain to 9 by the sixth pass, the strain hardening considerably reduces and the ratio of YS /UTS increases to 0.85, which is the highest value in this research work.

During the sixth pass of the DECLE process, the average grain size is significantly reduced and the final product contains an ultra-fine structure. Such structures, which are basically produced via SPD operations, involve very high dislocation densities. This property limits further congregation of dislocations during the supplementary tensile tests [34]. That is why the sixth pass DECLED sample represented the lowest elongation and strain hardening behavior. Similar observations were made after ECAP process at 373 K on the same aluminum alloy [35]. As the number of passes increased, both the ductility and strain hardening of the alloy decreased, whereas both the yield and ultimate strengths increased. It is also worthy to mention that very fine grains have a tendency to lose strain hardening behavior because they have very low capacity to accommodate the dislocations. Such materials possess a high potential for unstable plastic deformation and, eventually, losing a uniform elongation [35]. As mentioned previously, another reason for increase in strength after the sixth pass of the operation is the formation of grains with high angle boundaries within the microstructure of the material. This type of grains, compared with grains containing low angle boundaries, provide stronger barriers for dislocation movement. Consequently, the congregation of dislocation within the grains increases and this, in turn, results in significant growth in the strength of the material.

As can be observed in Table 1, in comparison with route A, route B is capable of providing greater strength and hardness values. This is in agreement with observations made by GUO et al [21] for DECLE of AZ31 magnesium alloy. Route B of DECLE process is nearly similar to route B_C in ECAP operation. It has been reported that, among different routes of ECAP process, route B_C is the best for attaining equiaxed and ultra-fined

microstructures. It is also claimed that the highest yield and ultimate strengths were achieved by using this route [36]. Therefore, it is reasonable that in the present investigation, route B has resulted in DECLED material with higher strength and hardness, in comparison with route A.

5 Conclusions

1) The hardness of AA5083 alloy increased from HV 88 for the annealed billet to HV 144 after the sixth pass. This significant improvement was mainly owing to severe plastic deformation accompanied by simultaneous reduction in the process temperature such that after the sixth pass, the average grain size is reduced to 200 nm.

2) It should be claimed that microstructural studies illustrated certain differences between the region just underneath the punch and other zones of the sample deformed through just the first pass. However, to compare the properties of the material after different passes, the same region of the sample was considered for hardness measurements and preparation of the tensile test specimens. Inspecting the hardness distribution in various directions and planes for this common region after different passes of the DECLE process, very good uniformity and homogeneity were observed within the products.

3) Simultaneous reduction in the process temperature and increase in the level of induced plastic strain resulted in high density of dislocations in the material. This provided a continuous and monotonic increase in both the yield and ultimate strengths. Even after the sixth pass of the process, no saturation in the strength occurred.

4) More pronounced strain hardening behavior is perceived for route A, compared with route B with similar test conditions. Therefore, route A involves less dislocation density in comparison with route B, because the greater the work hardening is, the lower the density of dislocations is. That is why greater strengths and hardness are noticed in route B.

5) From industrial point of view, DECLE process is capable of considerable strengthening of different

materials involving AA5083 aluminum alloy, especially when route B is employed. The present investigation showed that performing a 6-pass DECLE operation on AA5083, with route B and decreasing pass temperature resulted in improvements of 107%, 64% and 46% in YS, hardness and UTS, respectively.

Acknowledgements

The investigation described here was partially supported by the Iran National Science Foundation (INSF) with grant number 92014140. The authors appreciate the financial funding from this organization.

References

- [1] VALIEV R Z, LANGDON T G. Developments in the use of ECAP processing for grain refinement [J]. *Reviews on Advanced Materials Science*, 2006, 13: 15–26.
- [2] JIANG Shu-yong, ZHAO Ya-nan, ZHANG Yan-qiu, TANG Ming, LI Chun-feng. Equal channel angular extrusion of NiTi shape memory alloy tube [J]. *Transactions of Nonferrous Metals Society of China*, 2013, 23: 2021–2028.
- [3] SONG Jie, WANG Li-ming, ZHANG Xiao-ning, SUN Xiao-gang, JIANG Hong, FAN Zhi-guo, XIE Chao-ying, WU M H. Effects of second phases on mechanical properties and martensitic transformations of ECAPed TiNi and Ti–Mo based shape memory alloys [J]. *Transactions of Nonferrous Metals Society of China*, 2012, 22: 1839–1848.
- [4] JIANG Shu-yong, TANG Ming, ZHAO Ya-nan, HU Li, ZHANG Yan-qiu, LIANG Yu-long. Crystallization of amorphous NiTi shape memory alloy fabricated by severe plastic deformation [J]. *Transactions of Nonferrous Metals Society of China*, 2014, 24: 1758–1765.
- [5] JIANG Shu-yong, HU Li, ZHAO Ya-nan, ZHANG Yan-qiu, LIANG Yu-long. Plastic yielding of NiTi shape memory alloy under local canning compression [J]. *Transactions of Nonferrous Metals Society of China*, 2013, 23: 2905–2913.
- [6] VALIEV R Z, LANGDON T G. Principles of equal-channel angular pressing as a processing tool for grain refinement [J]. *Progress in Materials Science*, 2006, 51: 881–981.
- [7] RICHERT M, LIU Q, HANSEN N. Microstructural evolution over a large strain range in aluminum deformed by cyclic extrusion compression [J]. *Materials Science and Engineering A*, 1999, 260: 275–283.
- [8] PARDIS N, TALEBANPOUR B, EBRAHIMI R, ZOMORODIAN S. Cyclic expansion extrusion (CEE): A modified counterpart of cyclic extrusion compression (CEC) [J]. *Materials Science and Engineering A*, 2011, 528(25–26): 7537–7540.
- [9] MOHAMMED IQBAL U, SENTHIL KUMAR V S. An analysis on effect of multipass twist extrusion of AA6061 alloy [J]. *Materials & Design*, 2013, 50: 946–953.
- [10] BAYAT TORK N, PARDIS N, EBRAHIMI R. Investigation on the feasibility of room temperature plastic deformation of pure magnesium by simple shear extrusion process [J]. *Materials Science and Engineering A*, 2013, 560: 34–39.
- [11] ZHILYAEV A P, LANGDON T G. Using high pressure torsion for metal processing: Fundamentals and applications [J]. *Progress in Materials Science*, 2008, 53(6): 893–979.
- [12] WANG Q F, XIAO X P, HU J, XU W W, ZHAO X Q, ZHAO S J. An ultrafine-grained AZ31 magnesium alloy sheet with enhanced superplasticity prepared by accumulative roll bonding [J]. *Journal of Iron and Steel Research, International*, 2007, 14: 167–172.
- [13] HUANG J, ZHU Y T, ALEXANDER D J, LIAO X, LOWE T C, ASARO R J. Development of repetitive corrugation and straightening [J]. *Materials Science and Engineering A*, 2004, 371: 35–39.
- [14] KIM W J, KIM M J, WANG J Y. Superplastic behavior of a fine-grained ZK60 magnesium alloy processed by high-ratio differential speed rolling [J]. *Materials Science and Engineering A*, 2009, 527: 322–327.
- [15] HAN J H. A comparison of effects of pre-ECAR and post ECAR-aging on microstructure and strengthening in 7050 al alloy sheet [J]. *Materials Transactions*, 2010, 51(11): 2109–2112.
- [16] FARAJI G, YAVARI P, AGHDAMIFAR S, MOUSAVI-MASHHADI M. Mechanical and microstructural properties of ultrafine-grained AZ91 Magnesium alloy tubes processed via multi pass tubular channel angular pressing (TCAP) [J]. *Journal of Materials Science & Technology*, 2013, 30(2): 134–138.
- [17] TOTH L S, ARZAGHI M, FUNDENBERGER J J, BEAUSIR B, BUAZIZ O, ARRUFFAT-MASSION R. Severe plastic deformation of metals by high pressure tube-twisting [J]. *Scripta Materialia*, 2009, 60: 175–177.
- [18] FARSHIDI M H, KAZEMINEZHAD M. Deformation behavior of 6061 aluminum alloy through tube channel pressing: Severe plastic deformation [J]. *Journal of Materials Engineering and Performance*, 2012, 21: 2012–2099.
- [19] WANG J T, LI Z, WANG J, LANGDON T G. Principles of severe plastic deformation using tube high-pressure shearing [J]. *Scripta Materialia*, 2012, 67: 810–813.
- [20] KAMACH M, FURUKAWA M, HORITA Z, LANGDON T G. Equal channel angular pressing using plate samples [J]. *Materials Science and Engineering A*, 2003, 361: 258–266.
- [21] GUO W, WANG Q D, YE B, LIU M P, PENG T, LIU X T, ZHOU H. Enhanced microstructure homogeneity and mechanical properties of AZ31magnesium alloy by repetitive upsetting [J]. *Materials Science and Engineering A*, 2012, 540: 115–122.
- [22] TALEBANPOUR B, EBRAHIMI R, JANGHORBAN K. Microstructural and mechanical properties of commercially pure aluminum subjected to dual equal channel lateral extrusion [J]. *Materials Science and Engineering A*, 2009, 527: 141–145.
- [23] RAO V S, KASHYAP B P, PRABHU N, HODGSON P D. T-shaped equi channel angular pressing of Pb–Sn eutectic and its tensile properties [J]. *Materials Science and Engineering A*, 2008, 486(1): 341–349.
- [24] FAKHAR N, FERESHTEH-SANIEE F, MAHMUDI R. High strain-rate superplasticity of fine- and ultrafine-grained AA 5083 aluminum alloy at intermediate temperatures [J]. *Materials & Design*, 2015, 85: 342–348.
- [25] IWAHASI Y, WANG J, HORITA Z, NEMOTO M, LANGDON T G. Principle of equal channel angular pressing for the processing of ultra-fine grained materials [J]. *Scripta Materialia*, 1996, 35: 143–146.
- [26] TALEBANPOUR B, EBRAHIMI R. Upper-bound analysis of dual equal channel lateral extrusion [J]. *Materials & Design*, 2009, 30: 1484–1489.
- [27] WANG L Z, WANG J T, GUO C, CHEN J D. Observation of macroscopic shear band in aluminum based alloy during equal channel angular pressing [J]. *Transactions of Nonferrous Metals Society of China*, 2004, 14(5): 957–960.
- [28] HALIM H, WILKINSON D S, NIEWCZAS M. The portevin-Le chatelier (PLC) effect and shear band formation in an AA 5754 alloy [J]. *Acta Materialia*, 2007, 55: 4151–4160.
- [29] ZHOU H, YE B, WANG Q D, GUO W. Uniform fine microstructure and random texture of Mg–9.8Gd–2.7Y–0.4Zr magnesium alloy processed by repeated upsetting deformation [J]. *Materials Letters*,

- 2012, 83: 175–178.
- [30] KAPOOR R, CHAKRAVARTTY J K. Deformation behavior of an Ultra-fine grained Al–Mg alloy produced by equal channel angular pressing [J]. *Acta Materialia*, 2007, 55: 5408–5418.
- [31] CHANG S Y, LEE J G, PARK K T, SHIN D H. Microstructures and mechanical properties of equal channel angular pressed 5083 Al alloy [J]. *Materials Transactions*, 2001, 42(6): 1074–1080.
- [32] HUARTE B, LUIS C J, PUERTAS I, LEON J, LURI R. Optical and mechanical properties of an Al–Mg alloy processed by ECAP [J]. *Journal of Materials Processing Technology*, 2005, 162–163: 317–326.
- [33] GUO D, ZHANG Z, ZHANG G, LI M, SHI Y, MA T, ZHANG X. An extraordinary enhancement of strain hardening in fine grained zirconium [J]. *Materials Science and Engineering A*, 2014, 591: 167–172.
- [34] NING J L, COURTIS-MANARA E, KURMANAEVA L, GANEEV A V, VALIEV R Z, KUBEL C, IVANISENKO Y. Tensile properties and work hardening behaviors of ultrafine grained carbon steel and pure iron processed by high pressure torsion [J]. *Materials Science and Engineering A*, 2013, 581: 8–15.
- [35] CHANG S Y, AHN B D, HONG S K, KAMADO S, KOJIMA Y, SHIN D H. Tensile deformation characteristics of a nano-structured 5083 al alloy [J]. *Journal of Alloys and Compounds*, 2005, 386: 197–201.
- [36] DOBATKIN S V, SZPUNAR J A, ZHILYAEV A P, CHO J Y, KUZNETSOV A A. Effect of the route and strain of equal-channel angular pressing on structure and properties of oxygen-free copper [J]. *Materials Science and Engineering A*, 2007, 462: 132–138.

采用双通道等径侧面挤压法提高 AA5083 铝合金力学性能

N. FAKHAR¹, F. FERESHTEH-SANIEE¹, R. MAHMUDI²

1. Department of Mechanical Engineering, Faculty of Engineering,
Bu-Ali Sina University, Hamedan 65178, Iran;
2. School of Metallurgical and Materials Engineering,
College of Engineering, University of Tehran, Tehran, Iran

摘 要: 采用双通道等径侧面挤压剧烈塑性变形工艺提高 AA5083 铝合金的力学性能。采用多组实验研究路径类型(A 和 B 路径)和挤压道次对材料力学性能的影响。挤压道次为 6 道次, 挤压温度范围为 573~473 K, 采用金相、硬度测试和拉伸测试研究这些工艺参数的影响。硬度测试表明经 6 道次挤压后, 硬度提高了 64%, 且分布均匀。屈服强度和抗拉强度分别提高了 107%和 46%。这是由于晶粒的剧烈剪切变形和变形温度降低导致的晶粒细化。TEM 结果表明, 经 DECLE 6 道次变形后, 合金的平均晶粒尺寸从退火态的 100 μm 减小至 200 nm。对比研究了路径 A 和 B 的实验结果, 并得到一些重要结论。

关键词: AA5083 铝合金; 剧烈塑性变形; 双通道等径侧面挤压; 硬度均匀性

(Edited by Yun-bin HE)